Effect of inherent optical properties variability on the chlorophyll retrieval from ocean color remote sensing: an *in situ* approach

Hubert Loisel,[1,2,3,*] Bertrand Lubac,[4] David Dessailly,[1,2,3] Lucile Duforet-Gaurier,[1,2,3] and Vincent Vantrepotte[1,2,3]

[1]*Université Lille Nord de France*
[2]*ULCO, LOG, F-62930 Wimereux, France*
[3]*CNRS, UMR 8187, F-62930 Wimereux, France*
[4]*Université de Bordeaux 1, CNRS, UMR 5805, F- 33405 Talence, France*
*hubert.loisel@univ-littoral.fr

Abstract: The impact of the inherent optical properties (IOP) variability on the chlorophyll, *Chl*, retrieval from ocean color remote sensing algorithms is analyzed from an *in situ* data set covering a large dynamic range. The effect of the variability of the specific phytoplankton absorption coefficient, a_{phy}/Chl, specific particulate backscattering coefficient, b_{bp}/Chl, and colored detrital matter absorption to non-water absorption ratio, a_{cdm}/a_{nw}, on the performance of standard operational algorithms is examined. This study confirms that empirical algorithms are highly dependent on the specifics IOP values (especially b_{bp}/Chl and a_{cdm}/a_{nw}): *Chl* is over-estimated in waters with specific IOP values higher than averaged values, and *vice versa*. These results clearly indicate the necessity to account for the influence of the specific IOP variability in *Chl* retrieval algorithms.

©2010 Optical Society of America

OCIS codes: (280.4991) Passive remote sensing; (010.4450) Ocean optics; (010.1690) Color; (010.1030) Absorption; (010.1350) Backscattering.

References and links

1. J. E. O'Reilly, S. Maritorena, B. G. Mitchell, D. A. Siegel, K. L. Carder, S. A. Garver, M. Kahru, and C. R. McClain, "Ocean color chlorophyll algorithms for SeaWiFS," J. Geophys. Res. **103**(C11), 24,937–24,953 (1998).
2. T. S. Moore, J. W. Campbell, and M. D. Dowell, "A class-based approach to characterizing and mapping the uncertainty of the MODIS ocean chlorophyll product," Remote Sens. Environ. **113**(11), 2424–2430 (2009).
3. B. G. Mitchell, and O. Holm-Hansen, "Bio-optical properties of Antarctic Peninsula waters: Differentiation from temperate ocean models," Deep-Sea Res. **38**(8-9), 1009–1028 (1991).
4. A. Bricaud, H. Claustre, J. Ras, and K. Oubelkheir, "Natural variability of phytoplankton absorption in oceanic waters: Influence of the size structure of algal populations," J. Geophys. Res. **109**(C11), C11010 (2004), doi:10.1029/2004JC002419.
5. W. M. Balch, K. Kilpatrick, P. M. Holligan, D. Harbour, and E. Fernandez, "The 1991 coccolithophore bloom in the central north Atlantic II: relating optics to coccolith concentration," Limnol. Oceanogr. **41**(8), 1684–1696 (1996).
6. W. M. Balch, H. R. Gordon, B. C. Bowler, D. T. Drapeau, and E. S. Booth, "Calcium carbonate measurements in the surface global ocean based on Moderate-Resolution Imaging Spectroradiometer data," J. Geophys. Res. **110**(C7), C07001 (2005), doi:10.1029/2004JC002560.
7. S. Alvain, C. Moulin, Y. Dandonneau, H. Loisel, and F. M. Bréon, "A species-dependent bio-optical model of case 1 waters for global ocean color processing," Deep Sea Res. Part II Top. Stud. Oceanogr. **53**, 917–925 (2006).
8. M. Stramska, D. Stramski, S. Kaczmarek, D. B. Allison, and J. Schwarz, "Seasonal and regional differentiation of bio-optical properties within the north polar Atlantic," J. Geophys. Res. **111**(C8), C08003 (2006), doi:10.1029/2005JC003293.
9. K. L. Carder, S. K. Hawes, K. A. Baker, R. C. Smith, R. G. Steward, and B. G. Mitchell, "Reflectance model for quantifying chlorophyll-a in the presence of productivity degradation products," J. Geophys. Res. **96**(C11), 20599–20611 (1991).

10. D. A. Siegel, S. Maritorena, N. B. Nelson, M. J. Behrenfeld, and C. R. McClain, "Colored dissolved organic matter and its influence on the satellite-based characterization of the ocean biosphere," Geophys. Res. Lett. **32**(20), L20605 (2005), doi:10.1029/2005GL024310.
11. A. Morel, and B. Gentili, "The dissolved yellow substance and the shades of blue in the Mediterranean Sea," Biogeosciences **6**(11), 2625–2636 (2009).
12. C. A. Brown, Y. Huot, P. J. Werdell, B. Gentili, and H. Claustre, "The origin and global distribution of second order variability in satellite ocean color and its potential applications to algorithm development," Remote Sens. Environ. **112**(12), 4186–4203 (2008), doi:10.1016/j.rse.2008.06.008.
13. P. J. Werdell, and S. W. Bailey, "An improved in situ bio-optical data set for ocean color algorithm development and satellite data product validation," Remote Sens. Environ. **98**(1), 122–140 (2005).
14. H. Loisel, X. Mériaux, A. Poteau, L. F. Artigas, B. Lubac, A. Gardel, J. Caillaud, and S. Lesourd, "Analyze of the inherent optical properties of French Guiana coastal waters for remote sensing applications," J. Coast. Res. SI **56**, 1532–1536 (2009).
15. B. Lubac, and H. Loisel, "Variability and classification of remote sensing reflectance spectra in the eastern English Channel and southern North Sea," Remote Sens. Environ. **110**(1), 45–58 (2007).
16. A. Bricaud, M. Babin, A. Morel, and H. Claustre, "Variability in the chlorophyll-specific absorptioncoefficients of natural phytoplankton - analysis and parameterization," J. Geophys. Res. **100**(C7), 13321–13332 (1995).
17. R. A. Reynolds, D. Stramski, and B. G. Mitchell, "A chlorophyll-dependent semianalytical reflectance model derived from field measurements of absorption and backscattering coefficients within the Southern Ocean," J. Geophys. Res. **106**(C4), 7125–7138 (2001).
18. Y. Huot, A. Morel, M. S. Twardowski, D. Stramski, and R. A. Reynolds, "Particle optical scattering along a chlorophyll gradient in the upper layer of the eastern South Pacific Ocean," Biogeosciences **5**(2), 495–507 (2008).
19. H. R. Gordon, and A. Morel, "Remote assessment of ocean color for satellite visible imagery. A review, "p. 1-114. In R. T. Barber, C. N. K. Mooers, M. J. Bowman, and B. Zeizschel [eds.]. Lecture notes on coastal and estuarines studies. Springer-Verlag (1983).
20. H. Loisel, and A. Morel, "Light scattering and chlorophyll concentration in case 1 waters: A re-examination," Limnol. Oceanogr. **43**(5), 847–858 (1998).
21. D. A. Siegel, S. Maritorena, N. B. Nelson, and M. J. Behrenfeld, "Independence and Interdependencies Among Global Ocean Color Properties: Reassessing the Bio-Optical Assumption," J. Geophys. Res. **110**(C7), C07011 (2005b), doi:10.1029/2004JC002527.
22. A. Morel, "Are the empirical relationships describing the bio-optical properties of case 1 waters consistent and internally compatible?" J. Geophys. Res. **114**(C1), C01016 (2009), doi:10.1029/2008JC004803.
23. D. A. Siegel, S. Maritorena, N. B. Nelson, D. A. Hansell, and M. Lorenzi- Kayser, "Global distribution and dynamics of colored dissolved and detrital organic materials," J. Geophys. Res. **107**(C12), 3228 (2002), doi:10.1029/2001JC000965.
24. J. E. O'Reilly, S. Maritorena, D. A. Siegel, M. C. O'Brien, D. Toole, B. G. Mitchell, M. Kahru, *et al.*, "Ocean color chlorophyll a algorithms for SeaWiFS, OC2, and OC4: Version 4," In S. B. Hooker & E.R. Firestone (Eds.), SeaWiFS Postlaunch Calibration and Validation Analyses, Part 3, vol. 11. (pp. 9−23) Greenbelt, Maryland: NASA, Goddard Space Flight Center (2000).
25. R. J. Hyndman, and Y. Fan, "Sample Quantiles in Statistical Packages," Am. Stat. **50**(4), 361–365 (1996).
26. K. L. Carder, S. K. Hawes, K. A. Baker, R. C. Smith, R. G. Steward, and B. G. Mitchell, "Reflectance model for quantifying chlorophyll-a in the presence of productivity degradation products," J. Geophys. Res. **96**(C11), 20599–20611 (1991).
27. H. Claustre, A. Morel, S. B. Hooker, M. Babin, D. Antoine, K. Oubelkheir, A. Bricaud, K. Leblanc, B. Quéguiner, and S. Maritorena, "Is desert dust making oligotrophic waters greener," Geophys. Res. Lett. **29**(10), 1469 (2002), doi:10.1029/2001GL014056.
28. IOCCG, "Remote Sensing of Inherent Optical Properties: Fundamentals, Tests of Algorithms, and Applications," in *Reports of the International Ocean-Colour Coordinating Group, No. 5*, Z. P. Lee, ed. (IOCCG, Dartmouth, 2006).
29. S. Maritorena, D. A. Siegel, and A. R. Peterson, "Optimization of a semianalytical ocean color model for global-scale applications," Appl. Opt. **41**(15), 2705–2714 (2002).

1. Introduction

Retrieval of chlorophyll-a concentration, *Chl*, from ocean color remote sensing is traditionally performed using blue-to-green reflectance ratio, BGR [1]. This is mainly due to the fact that *Chl* (in $mg.m^{-3}$), a common pigment to all phytoplankton species, absorbs strongly in the blue and weakly in the green spectral domain. Empirical ocean color algorithms were then developed from *in situ* and simultaneous measurements of *Chl* and remote sensing reflectance, $R_{rs}(\lambda)$ (in sr^{-1}). $R_{rs}(\lambda)$ represents the ratio of the upwelling radiance to the downwelling irradiance above the sea surface at a given visible wavelength λ (in nm). These empirical algorithms are easy to develop but are by definition highly dependent on the data set used for

their development. While BGR exhibits a net decrease from oligotrophic (blue) to eutrophic (green) waters, a large statistical dispersion is however noticeable around this mean trend (Fig. 1). This pattern may considerably affect the accuracy of the *Chl* retrieval from space, which can be much beyond the nominal uncertainty of 35% [2].
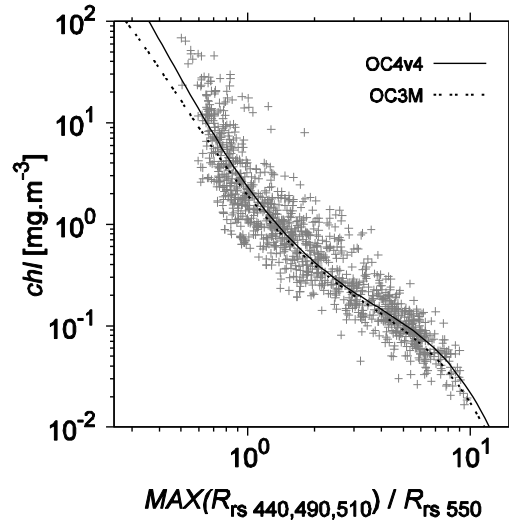

Fig. 1. Scatter plot of the chlorophyll concentration, *Chl*, as a function of blue to green reflectance ratio, BGR, from the whole *in situ* data set (N = 862). The solid and dashed curves represent the OC4v4 and OC3M algorithms, respectively.

While the noise in the correlation between BGR and *Chl* is partly related to uncertainties in *Chl* and $R_{rs}(\lambda)$ *in situ* measurements, natural variability of inherent optical properties (IOP) undeniably affects this relationship. Among IOP, which depend on the concentration and nature of the various optically-significant components in presence, the absorption (*a*) and backscattering (b_b) coefficients (both in m^{-1}) are related to R_{rs}: $R_{rs}(\lambda) \sim b_b(\lambda)/a(\lambda)$. While the first order variability of IOP is mainly driven by *Chl* in oceanic waters, the second order variability observed around the IOP vs. *Chl* relationships is directly related to the specific IOP variability. For a given chlorophyll concentration, variations in the absorption and backscattering spectra affect the spectral values of $R_{rs}(\lambda)$ and hence the BGR. For example, variations in algal community size structure modify, through the package effect, the phytoplankton absorption spectrum therefore affecting the remote sensing of phytoplankton pigments [3,4]. During coccolithophore blooms, coccolithes detached from the phytoplankton cells greatly contribute to increase b_b [5], therefore inducing an overestimation of the *Chl* derived from ocean color remote sensing [6]. Variation in the phytoplankton assemblages can also have a relevant impact, as large as 50%, on the *Chl* retrieval as pointed out by Alvain *et al*. [7] from ocean color remote sensing data. The respective proportion of phytoplankton, non-algal particles and colored dissolved organic matter also influences the amplitude and spectral behaviour of R_{rs}. For instance, Stramska *et al*. [8] have shown from *in situ* measurement performed in the north polar Atlantic that variations in the concentrations of detrital particles and accessory pigments may drastically affect the *Chl* retrieval. In the same way, absorption by colored dissolved organic matter and detrital particles may lead to large errors in the estimation of *Chl* loads [9–11]. Similar conclusions were recently reached by Brown *et al*. [12] who showed that the second order variability in the satellite ocean color signal for a given chlorophyll concentration is mainly explained by the amount of colored dissolved organic matter and particulate backscattering.

Previous studies have provided evidences that the estimation of *Chl* from ocean color remote sensing may be affected by IOP variability. These studies are generally based on local

in situ data sets or satellite remote sensing data which include many sources of errors. Indeed, uncertainties on the *Chl* retrieval from ocean color remote sensing have different origins: atmospheric correction errors, bio-optical algorithm uncertainties, mismatches in spatial scales, as well as *in situ* measurement errors. The aim of the present paper is to examine the origin of the scatter in the BGR vs. *Chl* relationship from an *in situ* data set covering a large dynamic range. The impact of the variability of different specific IOP on the *Chl* retrieval is addressed in order to identify and compare their respective influence.

2. Data and method

In this study we use the NOMAD data set [13] together with data collected during other oceanographic cruises occurring in the French Guyana coastal waters [14] and in the English Channel and North sea [15] which have been recently included in the NOMAD data set. Using this data set, covering oceanic and coastal waters, we analyse the impact of three specific IOP on the dispersion in the BGR vs. *Chl* relationship. The first one is the specific phytoplankton absorption coefficient at 443 nm (a_{phy}/Chl). A large natural variability in the a_{phy} vs. *Chl* relationship has long been pointed out. a_{phy}/Chl may indeed vary by a factor of about 4 for a given *Chl* concentration [16]. This biological noise is mostly driven by the average size of algal populations (i.e. package effect) rather than by the proportion of accessory pigments relative to *Chl* [4]. The second parameter is the specific particulate backscattering coefficient at 532 nm (b_{bp}/Chl). Field measurements performed in various oceanic areas have shown that b_{bp} exhibits a high variability (about a factor of 4) for a given chlorophyll concentration [17,18]. While the b_{bp}/Chl variability is driven by particle size distribution, refractive index and shape of the bulk particulate matter, the respective influence of each of these factors is still poorly known. The last specific IOP is the ratio of the colored detrital matter absorption coefficient, a_{cdm}, to the non-water absorption coefficient, a_{nw}, at 443 nm ($a_{nw} = a_{phy} + a_{cdm}$). The relative contribution of colored detrital matter absorption to non water absorption, which may drastically modify the spectral shape of R_{rs}, is highly variable in natural waters being dependent on various biogeochemical and physical processes.
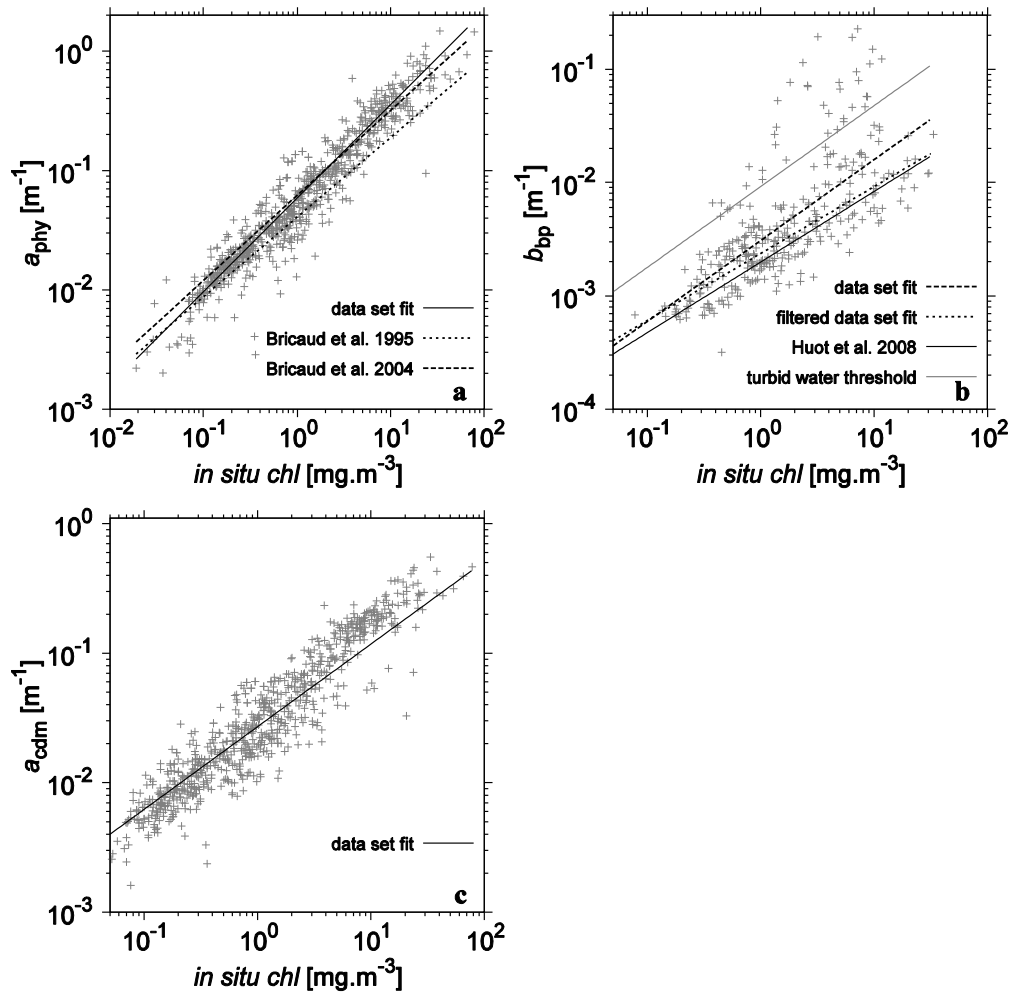
Fig. 2. (a) $a_{phy}(443)$ as a function of *Chl*. The solid curve represents the best fit for the 762 data points, and the dashed curves result from the algorithms of *Bricaud et al.* [4,16] as indicated. (b) $b_{bp}(530)$ as a function of *Chl*. The long dashed represents the best fit for the 323 data points, the short dashed curves represents the best fit for the 275 data points for which the very turbid waters have been disregarded, and the solid line results from the algorithm of *Huot et al*. [18]. (c) $a_{cdm}(443)$ as a function of *Chl*. The solid curve represents the best fit for the 762 data points.

The whole data set used in this study encompasses 862 pairs of (*Chl*, R_{rs}) data points for which one specific IOPs is at least available (760 are from NOMAD). Phytoplankton and colored detrital matter absorption measurements are available for 762 (*Chl*, BGR) data points, whereas particulate backscattering measurements are available for 323 (*Chl*, BGR) data points. This difference does not significantly affect the conclusions of this study since the b_{bp}/Chl, a_{phy}/Chl, and a_{cdm}/a_{nw} data points are distributed over roughly similar chlorophyll ranges. The proportion of data with relatively low chlorophyll concentration (Chl $\leq$ 0.5 mg.m^{-3}) is however lower in the b_{bp}/Chl data set (19%) than in the a_{phy}/Chl and a_{cdm}/a_{nw} data sets (36% for both). The median values of b_{bp}/Chl, a_{phy}/Chl, and a_{cdm}/a_{nw} are 0.0024 m^{2}mg^{-1}, 0.054 m^{2}mg^{-1}, and 0.61 respectively. The coefficient of variation (i.e. a ratio of standard deviation to the mean) for b_{bp}/Chl, a_{phy}/Chl, and a_{cdm}/a_{nw} are 152%, 53%, and 23%, respectively. $a_{phy}(443)$ increases with *Chl* according to a power law in good agreement with standard parameterisations [16]. A least square fit performed on the present data set provides

the following relationship: $a_{phy}(443) = 0.0543Chl^{-0.764}$(N = 762, r^2 = 0.91), which is very similar to the one developed by Bricaud *et al*. [4] on an large oceanic data set [Fig. 2(a)]. In the same way, the $b_{bp}(532)$-*Chl* dependency exhibits a non linear character, as expressed by the exponent 0.704:

$$b_{bp}(532) = 0.00299Chl^{0.704} \quad \left(N = 323, r^2 = 0.52\right) \tag{1}$$

This relationship is slightly modified by removing data collected in very turbid waters:

$$b_{bp}(532) = 0.00241Chl^{0.596} \quad \left(N = 275, r^2 = 0.70\right) \tag{2}$$

The threshold value for discriminating very turbid waters is fixed from Eq. (1) and Fig. 2(a), in a similar way as performed for the scattering coefficient [19,20]. In practice, stations with b_{bp}/*Chl* values greater than 0.009 $mg^{-1}m^2$ are classified as very turbid water. The non-turbid water relationship describe by Eq. (2) is very close to the one found by Huot *et al*. [17] from measurements performed in the upper layer of the eastern south Pacific ocean [Fig. 2(b)]. Similarly to $a_{phy}(443)$ and $b_{bp}(532)$ a relatively good relationship is also found between $a_{cdm}(443)$ and *Chl* [Fig. 2(c)]:

$$a_{cdm}(443) = 0.0265Chl^{0.63} \quad \left(N = 762, r^2 = 0.65\right) \tag{3}$$

This result is coherent with the study of Siegel *et al*. [21] performed on remote sensing ocean color data who found a significant determination coefficient (r = 0.58) between $a_{cdm}(443)$ and *Chl* (their Fig. 3 and Table 3). Note that the exponent 0.63 is similar to the one found by Morel [22] between the absorption by colored dissolved organic matter, a_{cdom}, and *Chl*, which is expected as a_{cdm} is dominated by a_{cdom} for nearly all the ocean [23]. The different observations reported here point out that the present data set, which covers a wide range of bio-optical conditions, is consistent with averaged relationships developed between IOP and *Chl* during the last decade.

The impact of the variability of these three specific IOP on the *Chl* retrieval is tested through the *Chl* vs BGR relationships described by the operational algorithms used for SeaWiFS (OC4.v4) and MODIS (OC3M) [24]. Each specific IOP sub data set is split into four equal parts computed according to Hyndman and Fan recommendation [25]. The first quartile cuts off the lowest 25% of the data. The corresponding sub data set is named DS1. The second quartile, which is equal to the median, cuts data set in half (DS2 and DS3), and third quartile cuts off highest 25% of data (DS4). The impact of the specific IOP on the *Chl* retrieval is evaluated through correlation analysis, root mean square log error, RMS, and average difference, AD. RMS is calculated as follows: RMS = $(\sum[\log(Chl_{retrieved})-\log(Chl_{in\ situ})]^2/N)^{0.5}$, and AD is defined as: AD = $(\sum[\log(Chl_{retrieved})-\log(Chl_{in\ situ})]/N$ (where N is the number of samples).

3. Results and discussion

The overall comparison between *in situ Chl* and OC4v4 or OC3M retrieved *Chl* (N = 862) indicates a relatively good agreement for the whole data set [Fig. 3(a)]. The RMS, AD, and r^2 values are 25.25%, 3.80%, and 0.88 using OC4v4 (N = 862), and 24.80%, −5.04%, and 0.88 using OC3M (N = 862). These results are consistent with the conclusions of Moore *et al.* [2] which were based on a much larger *in situ* data set. The scatter of the data points around the 1:1 line indicates that *Chl* may be over- or under-estimated by a factor of 2 within the whole chlorophyll range.
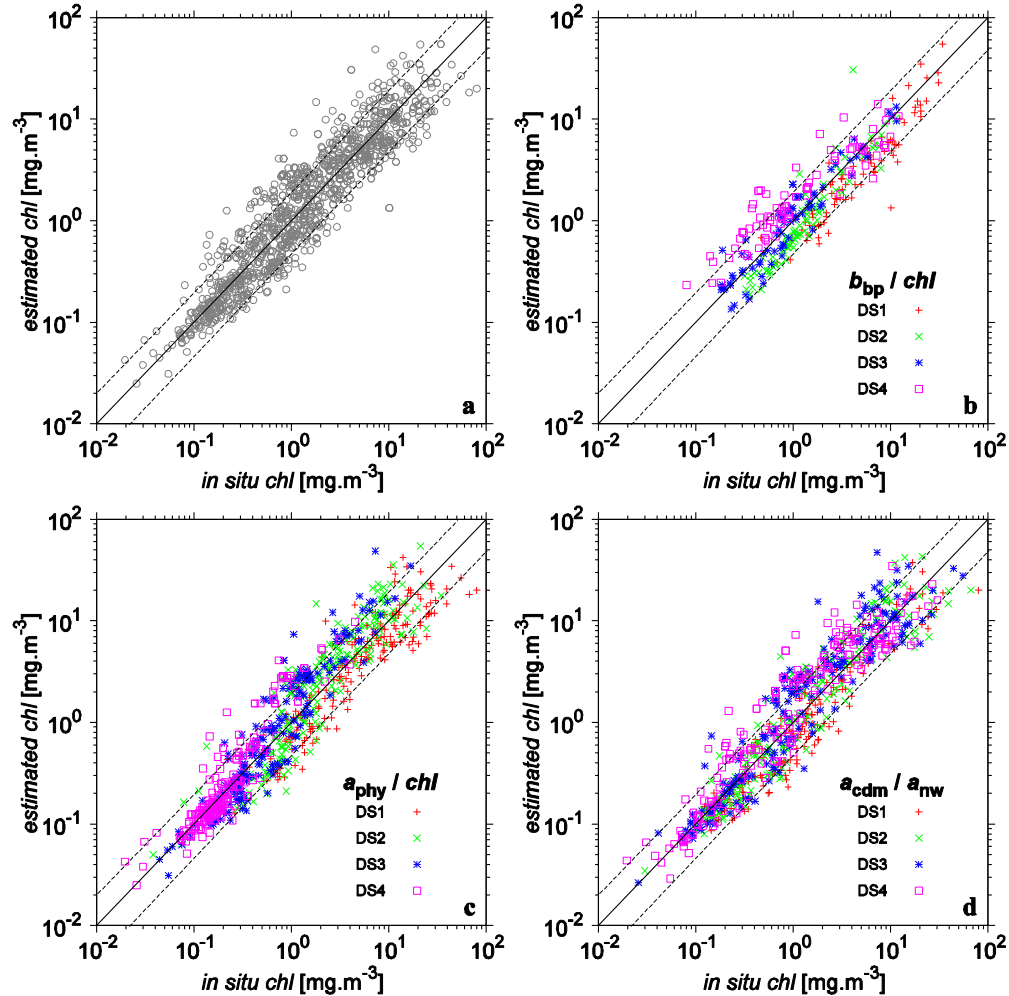
Fig. 3. (a) Comparison of the inversed (OC4v4) and measured *Chl* for the whole data set (N = 862). The solid line represents the 1:1 line, and the dashed lines the 1:2 and 2:1 lines. (b), (c), and (d) as in (a) but for the b_{bp}/*Chl* (N = 323), a_{phy}/*Chl* (N = 762), and a_{cdm}/a_{nw} (N = 762) data sets, respectively. The points belonging to DS1, DS2, DS3, and DS4 are represented as indicated for each specific IOP data set.

The comparison is now performed for the three specific IOP data sets to analyse the impact of the natural variability of IOP on the *Chl* retrieval accuracy [Figs. 3 (b), 3(c), 3(d)]. The RMS, AD, and r^2 values calculated for the data sets associated with each specific IOP are equivalent to those calculated for the whole data set (Table 1). For the three specific IOP data sets the relative error on the *Chl* retrieval may reach 100% over the whole *Chl* range (i.e. the data points on the 1:2 and 2:1 lines). While DS2 and DS3 are generally close to the 1:1 line of the *in situ* Chl vs satellite Chl relationships, this is not the case for DS1 and DS4. The points belonging to DS1 and DS4 are those for which the corresponding specific IOP values are respectively the lowest and greatest. The median and variation coefficient (in %) values of b_{bp}/*Chl*, a_{phy}/*Chl*, and a_{cdm}/a_{nw} are 0.0009 m^2mg^{-1}(37%), 0.0294 m^2mg^{-1} (25%), and 0.443 (18%) for DS1. The median values respectively jump to 0.0066 m^2mg^{-1} (94%), 0.098 m^2mg^{-1} (27%), and 0.757 (8%) for DS4. Therefore, the median b_{bp}/*Chl*, a_{phy}/*Chl*, and a_{cdm}/a_{nw} values vary respectively by a factor of 7.3, 3.3, and 1.7 between DS1 and DS4. When the very turbid data points are discarded from the b_{bp}/*Chl* data set, the median value of b_{bp}/*Chl* increases from

0.0008 m^{2}mg^{-1} (34%) to 0.0045 (24%) m^{2}mg^{-1} between DS1 and DS4 (a factor of 5.6). The average difference, which estimates the overall bias, clearly indicates that both OC4v4 and OC3M underestimate *Chl* (negative AD values) in DS1 and overestimate *Chl* (positive AD values) in DS4, whatever the specific IOP data set (Table 1). For instance, *Chl* is underestimated by 17.18% in DS1 and overestimated by 20.75% in DS4 for the b_{bp}/*Chl* data set and using OC4v4. Note that the AD values for the b_{bp}/*Chl* data set are similar for the non-very turbid data set (−17.2% for DS1 and 18.4% for DS4). Histograms showing the frequency distribution of the relative difference between the measured and estimated *Chl* also emphasize a significant shift from negative (under-estimation) to positive (over-estimation) values when the data set moves from DS1 to DS4 (Fig. 4). For instance, the median value of the relative difference between *in situ* and inversed OC4v4 *Chl* increases from −33% to 60% when b_{bp}/*Chl* increases between DS1 and DS4, respectively (same trend for OC3M). In contrast, this increase is lower for the two other specific IOP, as the median value of the relative *Chl* difference increases from −22% (−18.7) to 9.6% (27.4) when a_{phy}/*Chl* (a_{cdm}/a_{nw}) increases between DS1 and DS4. These results clearly indicate that *Chl* is underestimated by empirical algorithms in waters with specific IOP values "lower" than averaged values, and vice versa. Averaged values are calculated from the empirical relationships developed from *in situ* measurements of IOP and *Chl*.

Table 1. Root mean square log error, average difference, and regression coefficient values calculated between measured and predicted (with OC4v4 and OC3M) *Chl* for the whole data set (W), and the three specific IOP data set (for DS1 and DS4). The values for the non-very turbid data set are in bold

|	Whole OC4v4	Whole OC3M	b_{bp}/Chl OC4v4	a_{phy}/Chl OC4v4	a_{cdm}/a_{nw} OC4v4	b_{bp}/Chl OC3M	a_{phy}/Chl OC3M	a_{cdm}/a_{nw} OC3M
RMS-W	25.25	24.80	23.29/**21.8**	25.48	25.48	24.76/**24.47**	24.62	24.62
RMS-1			24.30/**23.2**	24.80	21.70	31.48/**32.28**	30.22	25.74
RMS-4			30.42/**27.0**	24.37	28.61	27.07/**23.93**	21.89	25.73
AD-W	3.80	−5.04	−0.59/**-3.02**	4.25	4.25	−8.26/**-10.2**	−4.06	−4.06
AD-1			−17.18/**-17.2**	−9.85	−9.14	−27.48/**-28.9**	−21.05	−15.73
AD-4			20.75/**18.4**	10.50	13.74	12.87/**13.4**	5.11	4.09
r^2-W	0.88	0.88	0.81/**0.84**	0.88	0.88	0.81/**0.83**	0.88	0.88
r^2-1			0.87/**0.89**	0.83	0.89	0.87/**0.88**	0.83	0.90
r^2-4			0.85/**0.72**	0.85	0.87	0.85/**0.72**	0.85	0.88

DS 1

DS 4
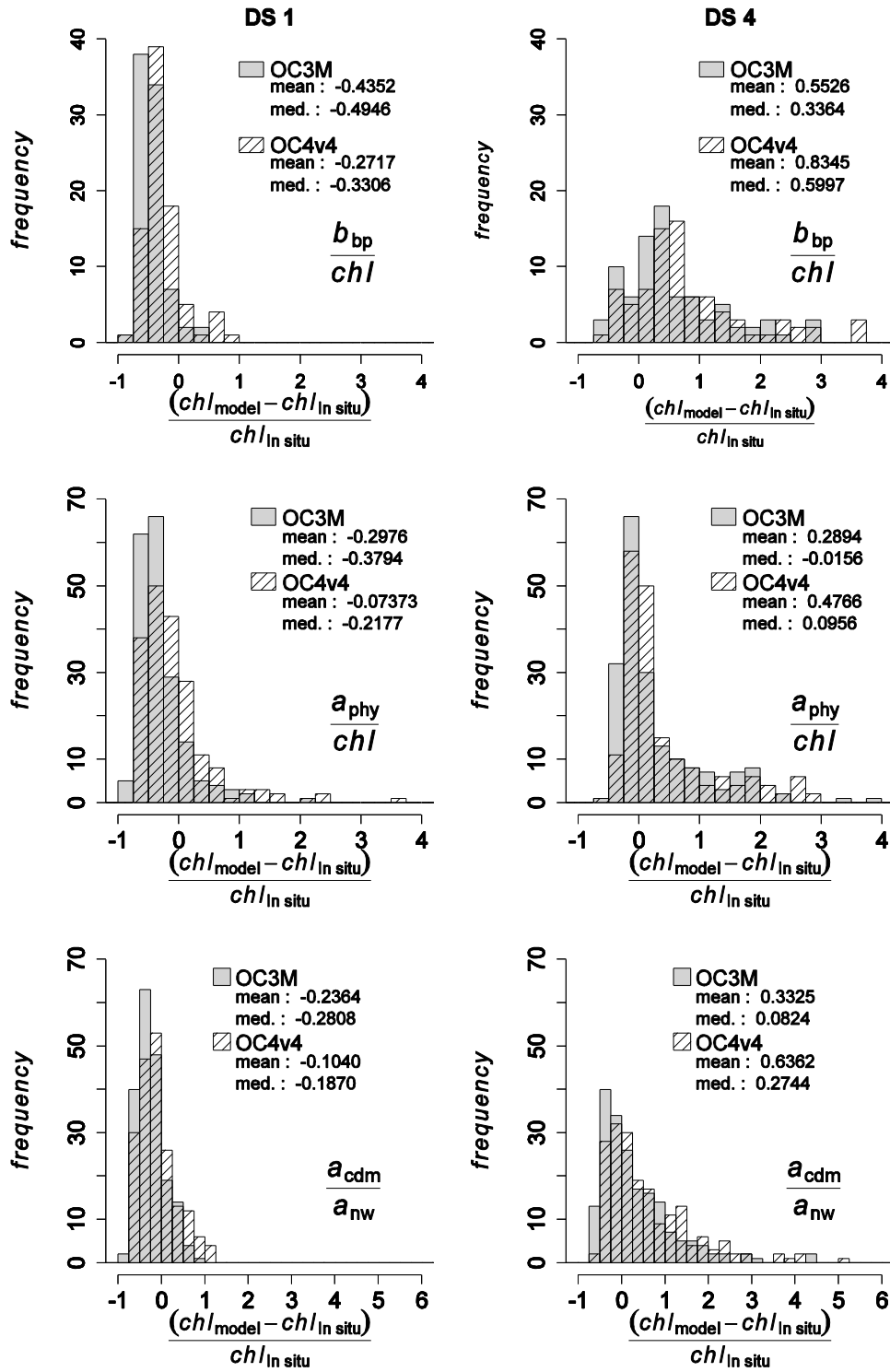
Fig. 4. Histograms of the *Chl* relative error calculated for each specific IOP data set and for DS1 (left panel) and DS4 (right panel) using OC4v4 and OC3M. The mean and median values are indicated.
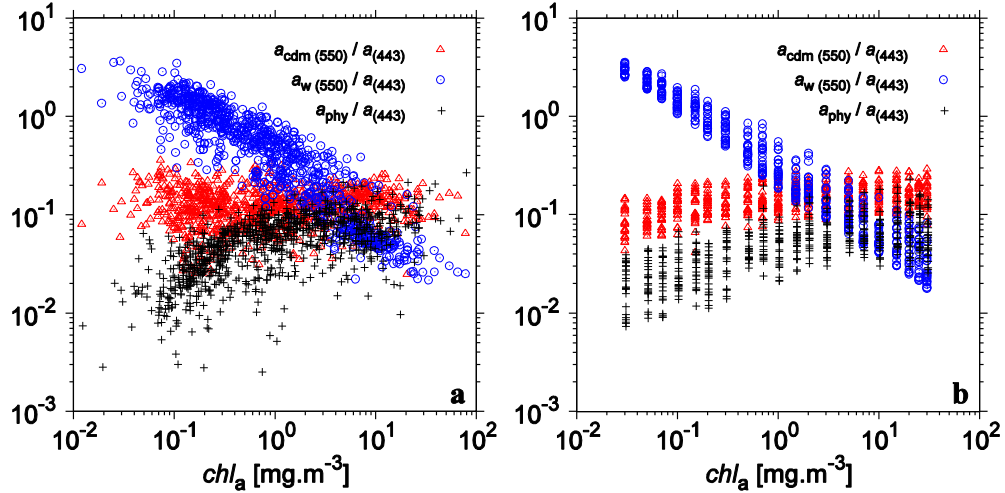
Fig. 5. $a_w(550)/a(440)$, $a_{cdm}(550)/a(440)$, and $a_{phy}(550)/a(440)$ as a function of *Chl* for (a) the present in situ data set (see text), and the synthetic data set [28].

Moreover, the latter features confirm that waters with higher b_{bp}/Chl, a_{phy}/Chl, or a_{cdm}/a_{nw} ratios will be seen greener by standard empirical algorithms. This is consistent with previous works performed on *in situ* or satellite measurements [11,26,27]. Due to differences in the spectral domains influenced by b_{bp}, a_{phy}, and a_{cdm} the three specific IOPs considered affect BGR in different ways. While a_{phy} and a_{cdm} mainly affect the blue spectral domain, b_{bp} influences the green region. Based on the present data set, one may additionally stress that the impact of b_{bp}/Chl on the BGR vs. *Chl* variability is much higher than that of a_{phy}/Chl and a_{cdm}/a_{nw}. This difference is mainly explained by the greater range of variability for b_{bp}/Chl when compared to that for a_{phy}/Chl and a_{cdm}/a_{nw}. Note however that for the same range of variability absorption by colored dissolved organic matter is expected to have a greater impact on the BGR vs. *Chl* relationship than the particulate backscattering coefficient [11]. The b_{bp}/Chl variability as well as the relative proportion between molecular and particular scattering directly affects the blue-to-green backscattering ratio, and consequently the BGR. Importantly, while the median value of a_{phy}/Chl varies twice as much as that of a_{cdm}/a_{nw} between DS1 and DS4, the respective impact of these two specifics IOP on the *Chl* retrieval is similar. This pattern may be explained by decomposing the green-to-blue absorption ratio (proportional to BGR) as: $(a_w(550) + a_{phy}(550) + a_{cdm}(550))/a(440)$. The evolution of $a_w(550)/a(440)$, $a_{cdm}(550)/a(440)$, and $a_{phy}(550)/a(440)$ is examined in function of changes in the *Chl* load using the present *in situ* data set [Fig. 5(a)] as well as a synthetic data set [Fig. 5(b)] generated in the frame of a working group on ocean-colour algorithm [28]. Based on these two different data sets $a_{cdm}(550)/a(440)$ is roughly constant over the whole chlorophyll range ($a_{cdm}(550)/a(440) \sim 0.13 \pm 0.05$ for the *in situ* data set), whereas $a_{phy}(550)/a(440)$ slightly increases with *Chl* according to: $\text{Log}(a_{phy}(550)/a(440)) = 0.27\text{Log}(Chl)-1.30$ ($r^2 = 0.38$) for the *in situ* data set. $a_{cdm}(550)/a(440)$ is therefore generally much higher than $a_{phy}(550)/a(440)$. For instance, $a_{cdm}(550)/a(440)$ is greater than $a_{phy}(550)/a(440)$ by a factor of 3.6 and 1.9 for *Chl* of 0.3 and 3.0 mg.m^{-3}, respectively. Hence, a given variation in $a_{cdm}(550)/a(440)$ has a greater effect on BGR than a variation of similar amplitude in $a_{phy}(550)/a(440)$.

Improvement of bio-optical algorithms dedicated to the *Chl* retrieval from ocean color remote sensing should account for specific IOP variability. Simultaneous retrieval of IOP and *Chl*, as already performed from semi-analytical algorithms (e.g. [29]), allows to partly take into account such variability (even though some specific IOP values have to be fixed in these

algorithms). Classification of R_{rs} spectra, prior to application of specific bio-optical algorithms, may also represent a valuable way to improve the *Chl* retrieval (e.g. [2,15]).

Acknowledgments